

See discussions, stats, and author profiles for this publication at: <https://www.researchgate.net/publication/49852174>

# Engineered Amp C $\beta$ -Lactamase as a Fluorescent Screening Tool for Class C $\beta$ -Lactamase Inhibitors

ARTICLE in ANALYTICAL CHEMISTRY · FEBRUARY 2011

Impact Factor: 5.64 · DOI: 10.1021/ac102595r · Source: PubMed

---

CITATION

1

---

READS

71

## 7 AUTHORS, INCLUDING:



[Emily Man Wah Tsang](#)

Okinawa Institute of Science and Technology

7 PUBLICATIONS 58 CITATIONS

[SEE PROFILE](#)

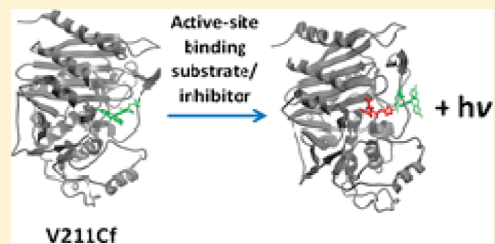
# Engineered Amp C $\beta$ -Lactamase as a Fluorescent Screening Tool for Class C $\beta$ -Lactamase Inhibitors

Man-Wah Tsang, Pak-Ho Chan, Pui-Kin So, Dik-Lung Ma, Chun-Wai Tsang, Kwok-Yin Wong,\*  
and Yun-Chung Leung\*

Department of Applied Biology and Chemical Technology, Central Laboratory of the Institute of Molecular Technology for Drug Discovery and Synthesis, The Hong Kong Polytechnic University, Hung Hom, Kowloon, Hong Kong, China

## S Supporting Information

**ABSTRACT:** Class C  $\beta$ -lactamases mediate antibiotic resistance in bacteria by efficiently hydrolyzing a broad range of  $\beta$ -lactam antibiotics. With their clinical significance and the lack of commercially available effective inhibitors, development of class C  $\beta$ -lactamase inhibitors has become one of the recent hot issues in the pharmaceutical industry. In this paper, we report the protein engineering of a fluorescent Amp C  $\beta$ -lactamase mutant designated as V211Cf for the in vitro screening of class C  $\beta$ -lactamase inhibitors. When a fluorescein (f) was incorporated at the entrance of the enzyme's active site (position 211), Amp C  $\beta$ -lactamase from *Enterobacter cloacae* P99 was tailor-made into a novel fluorescent biosensing protein that could display a fluorescence enhancement upon binding with its  $\beta$ -lactam substrates/inhibitors. With its catalytic activity close to the wild-type level, V211Cf can act as a "natural" fluorescent drug target for screening small binding molecules. In addition, V211Cf can allow specific detection for its active-site binding molecules and discriminate them from nondruglike molecules in the screen. Furthermore, V211Cf is amenable to a high throughput format. Taken together, V211Cf demonstrates the potential as an efficient tool for screening class C  $\beta$ -lactamase inhibitors and facilitates the discovery of therapeutics that can combat the clinically important class C  $\beta$ -lactamases.

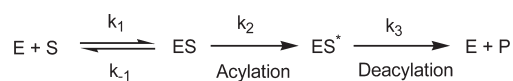


**$\beta$ -L**actam antibiotics, including penicillins and cephalosporins, have been the most popular antibiotics used in the treatment of bacterial infections over the past several decades. These antibiotics possess a functional moiety of the four-membered  $\beta$ -lactam ring, which can inactivate penicillin binding proteins (PBPs) through “irreversible” acylation and hence hinder them from synthesizing bacterial cell walls.<sup>1</sup> To combat  $\beta$ -lactam antibiotics, many bacteria have developed an effective defense mechanism involving the production of  $\beta$ -lactamases. These bacterial enzymes can hydrolyze the  $\beta$ -lactam ring into carboxylic acid as the product, thus rendering the antibiotic clinically inactive.

Among the four classes of  $\beta$ -lactamases (A–D),<sup>2</sup> class C enzymes (also known as cephalosporinases), which are often produced in Gram-negative bacteria, have caught considerable attention in recent years because of their ubiquity in certain pathogenic bacteria, broad spectrum, and ability to be produced in high levels in the bacterial cells. Unlike the most clinically prevalent class A counterparts, members in class C are usually more efficient in hydrolyzing cephalosporins,<sup>3,4</sup> which are potent antibiotics in the treatment of bacterial infections. These enzymes utilize Ser64 to undergo acylation with the carbonyl group of the  $\beta$ -lactam ring through a three-step process, which includes reversible substrate binding, acylation, and deacylation (Scheme 1).<sup>5,6</sup>

In addition, class C  $\beta$ -lactamases are less susceptible to many clinically useful  $\beta$ -lactamase inhibitors (e.g., clavulanic acid).<sup>7,8</sup> These

**Scheme 1.** Catalytic Pathway of  $\beta$ -Lactam Hydrolysis by Class C  $\beta$ -Lactamases<sup>a</sup>



<sup>a</sup> where E is the enzyme  $\beta$ -lactamase, S is an antibiotic substrate, ES is a noncovalent enzyme–substrate complex, ES\* is a covalent acyl enzyme–substrate complex, and P is the product.

alarming catalytic properties have complicated the treatment of bacterial infections involving the production of class C  $\beta$ -lactamases. With the great clinical impact of these problematic enzymes, extensive efforts have been directed to the development of new drugs that can inactivate class C  $\beta$ -lactamases effectively.<sup>9-15</sup>

Due to such a high demand for developing new therapeutics to target class C  $\beta$ -lactamases, high-throughput screening undoubtedly advanced the discovery of potential drug candidates from chemical libraries. However, this strategy is challenged by its susceptibility to false-positive hits.<sup>16</sup> In the situation of in vitro screening of class C  $\beta$ -lactamase inhibitors, false-positive hits are often the result of the

**Received:** October 20, 2010

**Accepted:** January 27, 2011

**Published:** February 21, 2011

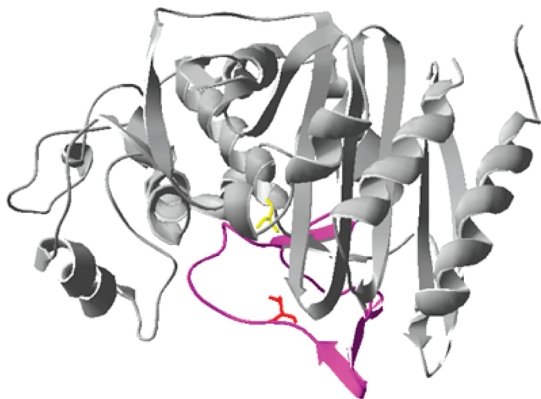


**Figure 1.** Structure of the P99  $\beta$ -lactamase (PDB: 1XX2). The Val211 and Ser64 residues are shown in red and yellow, respectively. Note that Val211 is located in the long loop (shown in magenta) close to the active site of the enzyme, with its side chain pointing toward the active site space.

formation of colloid aggregates because many compounds have a high propensity to form aggregates under aqueous conditions, which inhibit  $\beta$ -lactamase activity through a nonspecific mechanism (e.g., protein adsorption or absorption).<sup>17–21</sup> However, the conventional spectrophotometric method, which has been routinely used to detect  $\beta$ -lactamase activity,<sup>22</sup> is unable to differentiate between active-site-binding compounds (true positive drugs) and nondruglike aggregation-prone compounds (false positive drugs). In a recent high-throughput screen for class C  $\beta$ -lactamase inhibitors, a detergent-based counter-screen<sup>23</sup> revealed that 95% of the hits were false positive due to aggregate formation.<sup>24</sup> The dominant artifactual hits in the screen hit list often mislead drug discovery teams, thus leading to a huge waste of capital and resources. With this regard, it is highly desirable to develop a reliable high-throughput screening tool that can identify active-site-binding drug candidates against class C  $\beta$ -lactamases *in vitro*.

Recently, we have successfully constructed a fluorescent biosensor for  $\beta$ -lactam antibiotics from a nonallosteric class A  $\beta$ -lactamase.<sup>25</sup> In that work, we strategically impaired the activity of the enzyme through protein engineering and attached an environment-sensitive fluorophore to the flexible  $\Omega$ -loop close to the active site. The attached fluorophore can sense the environmental change induced by antibiotic binding and give fluorescence changes.<sup>26</sup> Owing to the structural and functional similarities and the common catalytic mechanism shared between class A and class C  $\beta$ -lactamases,<sup>27–29</sup> the encouraging results of the class A biosensor prompted us to apply the “active-site-labeling” approach to develop a novel fluorescent molecular drug target from the *Enterobacter cloacae* P99 AmpC  $\beta$ -lactamase (a class C  $\beta$ -lactamase) for *in vitro* drug screening. Here, the enzyme is labeled with a fluorescein in the close proximity to its active site so as to enable it to fluorescently respond to the drug binding event at the active site. Differing from the design of the class A  $\beta$ -lactamase biosensor, in the present work, the catalytic activity of the fluorescent P99 AmpC  $\beta$ -lactamase is intended to be maintained so that the enzyme can act as a “natural” molecular drug target. To achieve these purposes, in our design, the Val211 residue of the cysteine-free P99 enzyme was replaced by a cysteine, and subsequently, this unique Cys residue was labeled with an environment-sensitive fluorescein-5-maleimide. This residue was chosen for the following reasons: (1) Val211 is located in the long  $\Omega$ -loop (close to the active site), which can allow the attached fluorophore to sense the environmental change induced by the drug binding in the active site (Figure 1). Moreover, the flexible nature of the  $\Omega$ -loop can reduce the possible steric effect of the attached

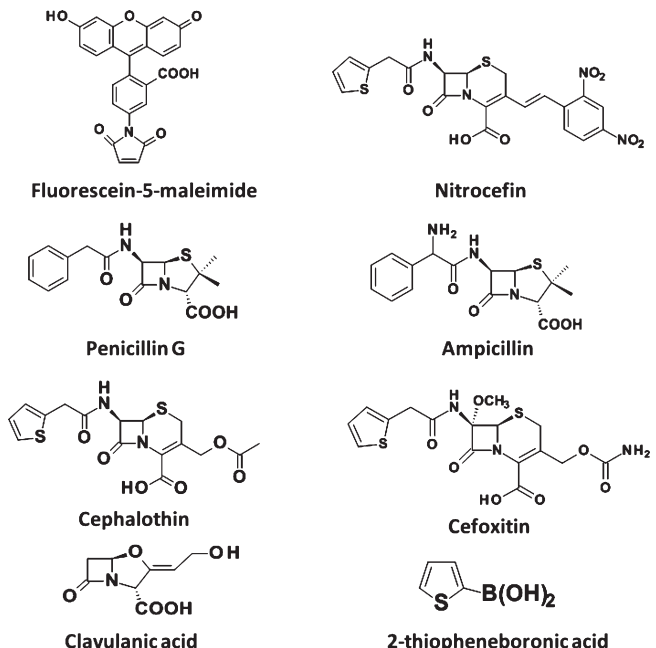


**Figure 2.** Structures of the  $\beta$ -lactam antibiotics (penicillin G, ampicillin, cephalothin, cefoxitin, nitrocefin),  $\beta$ -lactamase inhibitors (clavulanic acid, 2-thiopheneboronic acid), and fluorescein-5-maleimide used in this study.

fluorophore. (2) Val211 is a noncatalytic residue,<sup>30</sup> and hence, the catalytic activity of the V211C mutant is expected to be close to that of the wild-type enzyme. (3) Val211 is highly conserved in class C  $\beta$ -lactamases and can, therefore, serve as a “generic” site for fluorophore labeling in the development of fluorescent drug targets with other clinically relevant class C  $\beta$ -lactamases.

Our studies have shown that the labeled V211C mutant mimics the wild-type P99 enzyme in terms of catalytic properties toward antibiotic substrates and inhibitors. Moreover, the labeled mutant can fluorescently respond to the drug binding event in the active site rather than the nonspecific binding and irrelevant inhibition by aggregate-prone molecules. Taken together, these observations highlight the value of this fluorescent class C enzyme in *in vitro* drug screening.

## EXPERIMENTAL SECTION

**Chemicals.** Penicillin G, cephalothin, cefoxitin, chloramphenicol, kanamycin, glucose, sodium chloride, Tris-HCl, potassium dihydrogenphosphate, ammonium acetate, myoglobin (from horse heart), and hen egg-white lysozyme were purchased from Sigma (St. Louis, MO). Ampicillin was purchased from USB (Cleveland, OH). Congo red was obtained from BDH (Poole, UK). Nitrocefin was purchased from Becton Dickinson Company (Cockeysville, Md.). Clavulanic acid was a gift from Prof. Yoshikazu Ishii of Toho University, Japan. 2-Thiopheneboronic acid was obtained from Sigma (St. Louis, MO). Fluorescein-5-maleimide was purchased from Molecular Probes Inc. (Eugene, O.R.). Brain heart infusion (BHI) and yeast extract were obtained from Oxoid Ltd. (Nepean, Ontario, Canada). The chemical structures of fluorescein-5-maleimide,  $\beta$ -lactam antibiotics, and  $\beta$ -lactamase inhibitors used in this study are shown in Figure 2.

**Protein Expression and Purification.** Both the *E. cloacae* P99  $\beta$ -lactamase and the V211C mutant of this enzyme were expressed in *Bacillus subtilis* strain 1A304 ( $\phi$ 10SMU331) as N-terminally histidine-tagged ((His)<sub>6</sub>-tagged) recombinant proteins.<sup>31</sup> As the *Bacillus subtilis* strain transformed with the

$\beta$ -lactamase gene contains a chloramphenicol selective marker; the bacterial strain was streaked on an agar plate containing 5  $\mu\text{g}/\text{mL}$  chloramphenicol, and the plate was incubated at 37 °C for 24 h to select the  $\beta$ -lactamase gene containing bacterial species. A few single bacterial colonies from the agar plate were inoculated into 100 mL of sterile BHY medium (37 g/L BHI and 5 g/L yeast extract), which was then incubated at 37 °C with shaking at 300 rpm overnight (about 11–12 h). The overnight inoculum was subcultivated in sterile BHY medium at a dilution factor of 1:20 and grown at 37 °C with shaking at 300 rpm. When the OD<sub>600</sub> value reached 3.0–3.5, protein expression was induced by shaking the bacterial culture in a water bath at 50 °C for 5 min. After induction of protein expression, the culture was allowed to grow at 37 °C with shaking at 300 rpm for another 5 h, and then, the bacterial cells were harvested by centrifugation at 9000 rpm and 4 °C for 20 min.

Prior to purification, the cell pellet was resuspended in solubilization buffer and then lysed by lysozyme treatment and sonication. Afterward, the bacterial lysate was collected by centrifugation at 10 000 rpm and 4 °C for 1 h. With the exploitation of the ability of histidine to bind chelated transition metal ions, such as nickel ( $\text{Ni}^{2+}$ ), nickel affinity chromatography was applied to purify the (His)<sub>6</sub>-tagged protein. The affinity chromatography was performed on an Amersham-Pharmacia ÄKTA FPLC system (Amersham-Pharmacia Biotech Inc., Piscataway, NJ). The clarified cell lysate was loaded onto a  $\text{Ni}^{2+}$ -charged 5 mL HiTrap chelating column (Amersham-Pharmacia Biotech Inc.) pre-equilibrated with start buffer (20 mM sodium phosphate buffer, 0.5 M NaCl, pH 7.4). The column was then washed with 6 column volumes of the same buffer, and the (His)<sub>6</sub>-tagged enzyme was eluted by a linear gradient of 0–0.2 M imidazole. Fractions containing the enzyme were pooled and then dialyzed against 20 mM potassium phosphate buffer (pH 7.4) at 4 °C. All the enzymes were judged to be >95% pure by SDS-PAGE. For long-term storage, the purified enzymes were buffer-exchanged with 20 mM NH<sub>4</sub>HCO<sub>3</sub> (pH 8.0) at 4 °C, lyophilized and stored at –20 °C.

**Protein Labeling.** The lyophilized V211C mutant was dissolved in 50 mM potassium phosphate buffer (pH 7.0). A 20 mM stock solution of fluorescein-5-maleimide was prepared by dissolving the fluorophore in dimethylformamide. A 10-fold molar excess of fluorescein-5-maleimide was added to the protein solution, followed by shaking at 300 rpm in the dark for 30 min. Afterward, excess dye was removed by dialysis with 50 mM potassium phosphate buffer or by centrifugation using an Amicon Ultra-15 (NMWL = 10,000) centrifugal filter device. The labeled mutant was then stored at –80 °C. The labeling reaction of the V211C mutant with fluorescein-5-maleimide was examined by sodium dodecyl sulfate-polyacrylamide gel electrophoresis (SDS-PAGE).

**Fluorescence Measurements.** A 5  $\mu\text{L}$  aliquot of 10  $\mu\text{M}$  V211Cf (in 50 mM phosphate buffer, pH 7) was first mixed with 445  $\mu\text{L}$  of 50 mM phosphate buffer (pH 7.0) in a quartz cuvette of a 1 cm path length. A series of 1, 10, 100, 1000, and 10 000  $\mu\text{M}$  antibiotic samples (penicillin G, ampicillin, cephalothin, and cefoxitin) were prepared as the stock solutions (in 50 mM phosphate buffer, pH 7.0). A 5  $\mu\text{L}$  portion of the antibiotic stock solution was then added to the enzyme solution to give a reaction mixture containing the desired antibiotic concentration (0.1, 1, 10, 100, and 1000  $\mu\text{M}$ ) and 0.1  $\mu\text{M}$  V211Cf. The reaction mixture was mixed immediately, and the fluorescence signal was recorded using a Perkin-Elmer LS50B spectrofluorimeter. Both excitation and emission slit widths were 5 nm, and the sample was

excited at 498 nm. All fluorescence measurements were performed at 20 °C.

For stopped-flow fluorescence measurements, a stopped-flow instrument equipped with a fluorescence readout was used (Applied Photophysics SX.18MV-R, Leatherhead, UK). Both excitation and emission slit widths were 5 nm. The sample of V211Cf (0.1  $\mu\text{M}$ ) with various concentrations (0.1, 1, 10, and 100  $\mu\text{M}$ ) of the antibiotics (in 50 mM potassium phosphate buffer, pH 7.0) was excited at 498 nm, and the fluorescence signal was recorded at 517 nm. All stopped-flow fluorescence measurements were carried out at 20 °C.

For high-throughput drug screening experiments, the fluorescence signal changes of V211Cf with the inhibitors (clavulanic acid and 2-thiopheneboronic acid) were monitored using a FLUOStar Galaxy microplate reader equipped with two sample injectors (BMG LABTECH, Germany). The excitation and emission filters were 485 and 520 nm, respectively. A 96-well polystyrene microtiter plate (Corning Costar) was used as the sampler. The inhibitors (1 mM)/antibiotics (0.1 mM) were added to the V211Cf mutant (0.1  $\mu\text{M}$ ) in 50 mM potassium phosphate buffer (pH 7.0) at an injection speed of 310  $\mu\text{L}/\text{s}$  using the sample injectors. All the fluorescence measurements were performed at 20 °C.

**Detection of Covalent Acyl Enzyme–Substrate Complexes.** Formation of covalent acyl enzyme–substrate complexes between V211Cf and cefoxitin was monitored by electrospray ionization (ESI)-MS and fluorescence spectroscopy. The enzyme–substrate reaction was initiated by mixing 500  $\mu\text{L}$  of 3  $\mu\text{M}$  V211Cf in 50 mM potassium phosphate buffer (pH 7.0) with 500  $\mu\text{L}$  of 20  $\mu\text{M}$  cefoxitin in 50 mM potassium phosphate buffer (pH 7.0). At desired time intervals, 100  $\mu\text{L}$  portions of the reaction mixture were withdrawn and added into 100  $\mu\text{L}$  of quenching agent, which was composed of 8% formic acid in acetonitrile (CH<sub>3</sub>CN). The resulting quenched reaction mixtures composed of phosphate buffer/CH<sub>3</sub>CN (1:1 v/v) containing 4% formic acid (pH ~ 2) were exchanged into ammonium acetate buffer with 2% formic acid prior to ESI-MS analysis. The resulting ESI spectrum was found to show two major peaks (A and B) attributed to the free enzyme E and the enzyme–substrate complex ES\*, respectively. The relative amount of ES\* can be expressed as the ratio of the amount of ES\* to the total amount of the enzyme,  $[\text{ES}^*]/[\text{E}_{\text{total}}]$ , where  $[\text{ES}^*]$  is the peak area of peak B and  $[\text{E}_{\text{total}}] (= [\text{E}] + [\text{ES}^*])$  is the sum of peak areas of peak A and B in the transformed ESI mass spectrum. For comparison, parallel stopped-flow fluorescence measurement was also performed by adding 1.5  $\mu\text{M}$  V211Cf with 10  $\mu\text{M}$  cefoxitin in 50 mM postassium phosphate buffer (pH 7.0), using a stopped-flow instrument equipped with a fluorescence readout device (Applied Photophysics SX.18MV-R, Leatherhead, UK). The sample was excited at 498 nm, and the fluorescence signal was monitored at 517 nm. Both excitation and emission slit widths were 5 nm.

## ■ RESULTS AND DISCUSSION

**Fabrication and Characterization of V211Cf.** To fabricate V211Cf, a cysteine residue was first introduced to substitute Val211 of the P99 *E. cloacae*  $\beta$ -lactamase via site-directed mutagenesis to give the V211C mutant. Then V211C mutant protein was produced in *B. subtilis* and purified to more than 95% homogeneity as visualized in a Coomassie blue-stained SDS polyacrylamide gel. Afterward, the purified V211C mutant was

**Table 1.** Kinetic Parameters for the Hydrolysis of Penicillin G, Ampicillin, Cephalothin, and Cefoxitin by the Wild-Type P99 Enzyme, V211C, and V211Cf

		Wild-type	V211C	V211Cf
Penicillin G	$K_m$ ( $\mu\text{M}$ ) <sup>a</sup>	$1.6 \pm 0.1$	$1.8 \pm 0.6$	$7.9 \pm 0.6$
	$k_{\text{cat}}$ ( $\text{s}^{-1}$ ) <sup>b</sup>	$10.7 \pm 1$	$14.5 \pm 0.5$	$4.5 \pm 0.5$
	$k_{\text{cat}}/K_m$ ( $\text{M}^{-1}\text{s}^{-1}$ )	$(6.7 \pm 0.8) \times 10^6$	$(2.5 \pm 0.9) \times 10^6$	$(5.7 \pm 0.8) \times 10^5$
Ampicillin	$K_m$ ( $\mu\text{M}$ ) <sup>a</sup>	$0.8 \pm 0.06$	$1.0 \pm 0.06$	$9.1 \pm 0.5$
	$k_{\text{cat}}$ ( $\text{s}^{-1}$ ) <sup>b</sup>	$0.3 \pm 0.006$	$0.2 \pm 0.004$	$0.2 \pm 0.002$
	$k_{\text{cat}}/K_m$ ( $\text{M}^{-1}\text{s}^{-1}$ )	$(3.8 \pm 0.3) \times 10^5$	$(2 \pm 0.1) \times 10^5$	$(2 \pm 0.1) \times 10^4$
Cephalothin	$K_m$ ( $\mu\text{M}$ )	$9.1 \pm 0.7$	$26 \pm 1$	$64 \pm 6$
	$k_{\text{cat}}$ ( $\text{s}^{-1}$ )	$118 \pm 2$	$54 \pm 1$	$47 \pm 2$
	$k_{\text{cat}}/K_m$ ( $\text{M}^{-1}\text{s}^{-1}$ )	$(1.3 \pm 0.1) \times 10^7$	$(2.1 \pm 0.1) \times 10^6$	$(7.3 \pm 0.8) \times 10^5$
Cefoxitin	$K_m$ ( $\mu\text{M}$ ) <sup>a</sup>	$0.1 \pm 0.009$	$0.2 \pm 0.06$	$0.4 \pm 0.08$
	$k_{\text{cat}}$ ( $\text{s}^{-1}$ ) <sup>b</sup>	$0.08 \pm 0.004$	$0.05 \pm 0.004$	$0.02 \pm 0.004$
	$k_{\text{cat}}/K_m$ ( $\text{M}^{-1}\text{s}^{-1}$ )	$(8 \pm 0.8) \times 10^5$	$(2.5 \pm 0.8) \times 10^5$	$(5 \pm 1) \times 10^4$

<sup>a</sup>  $K_m$  values were measured as  $K_i$  values using nitrocefin as a reporter substrate. <sup>b</sup>  $k_{\text{cat}}$  values were obtained with saturating concentration (100  $\mu\text{M}$ ) of substrates.

labeled with a fluorescein molecule via thiol reaction between maleimide and the thiol group of the cysteine residue. Because the wild-type P99  $\beta$ -lactamase contains no cysteine,<sup>32</sup> the incorporated unique cysteine residue can ensure site-specific attachment of the fluorescein molecule to the V211C mutant via thiol reaction. The labeling reaction was monitored by electrospray ionization mass spectrometry (ESI-MS). For the wild-type and V211C enzymes, the measured mass values of these proteins are in good agreement with the theoretical mass values calculated from their amino acid sequences (Table S1, Supporting Information). In the case of the V211Cf mutant, the measured mass value of this labeled mutant is larger than the theoretical mass value by about 23 Da, a mass value consistent with that of a sodium ion. This mass difference can be explained by the formation of protein/sodium adducts which is a common phenomenon under ESI conditions.<sup>33</sup> Analysis of the measured mass values of V211C and V211Cf indicated that there is a mass difference of 450 Da between these two proteins. This mass difference is very consistent with the total mass value of fluorescein-5-maleimide plus a sodium ion (MW = 427 + 23 Da), confirming that V211C mutant was tethered with the fluorescein molecule in a 1:1 ratio. Moreover, while the ESI mass spectrum of V211Cf displays a strong peak corresponding to the V211Cf/ $\text{Na}^+$  adduct, a mass peak corresponding to the unlabeled V211C mutant was not observed in this mass spectrum (Figure S1, Supporting Information). Therefore, the V211C mutant can be effectively labeled with fluorescein in the presence of a 10-fold molar excess of fluorescein-5-maleimide.

Kinetic parameters of turnover of various  $\beta$ -lactam antibiotics by V211Cf were determined and compared with those values of parental wild-type and V211C enzymes (Table 1). In general, the wild-type, V211C, and V211Cf demonstrate similar kinetic values. For the  $K_m$  values, the magnitude of values is as follows: V211Cf > V211C > wild-type. As Val211 of the wild-type enzyme is situated at the entrance of the active site pocket, this trend in  $K_m$  values can be reasoned by the steric hindrance at the active site that may be imposed by the cysteine substitution and fluorophore coupling at position 211. However, the differences in  $K_m$  values of wild-type, V211C, and V211Cf mutants are small (<10-fold). This reveals that steric hindrance resulting from cysteine replacement and fluorophore attachment does not cause significant influences on substrate binding to the enzyme. Regarding

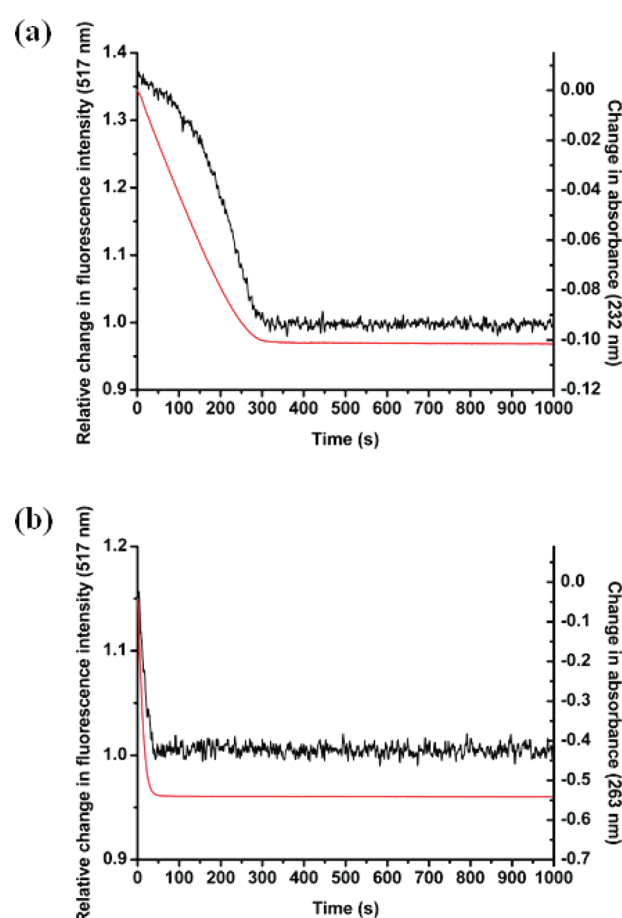


**Figure 3.** Time course of the hydrolysis of penicillin G and cephalothin by V211Cf monitored by UV absorption and fluorescence measurements. Plots of the time-resolved fluorescence signal at 517 nm (in black line) and the time-resolved UV absorbance at 232 nm for penicillin G and 263 nm for cephalothin (in red line) obtained from the hydrolysis of penicillin G and cephalothin (0.1 mM) by V211Cf (0.1  $\mu\text{M}$ ) are shown in (a) and (b), respectively.

the catalytic activities of the enzymes, the  $k_{\text{cat}}$  values of V211C and V211Cf are, in general, close to that of the wild-type enzyme. The  $k_{\text{cat}}$

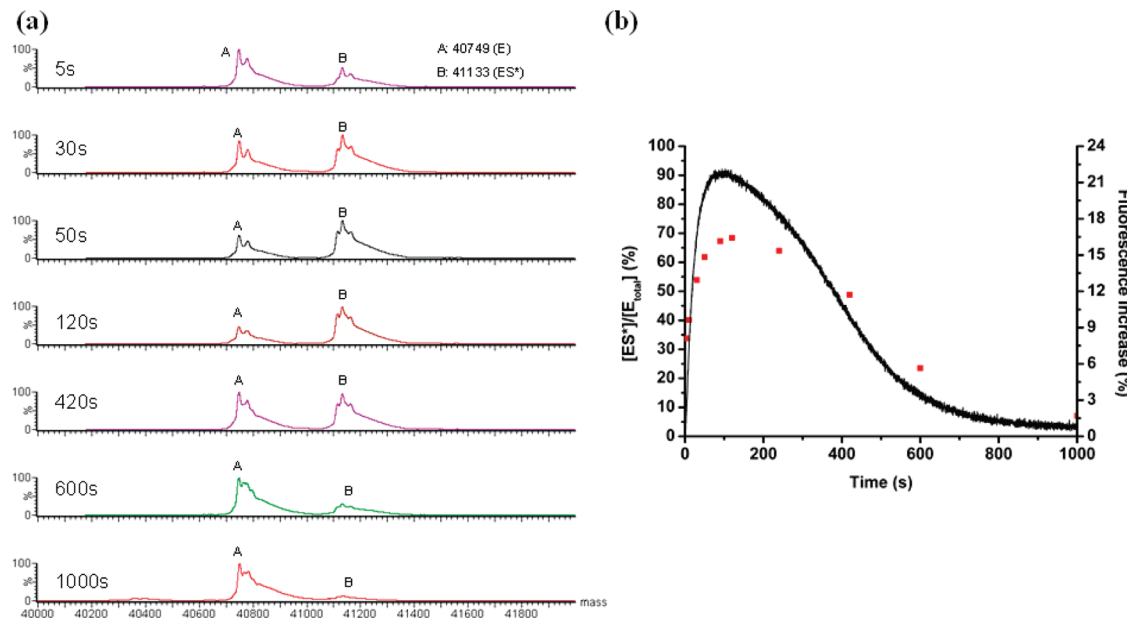


**Figure 4.** Binding of V211Cf ( $1.5 \mu\text{M}$ ) with cefoxitin ( $10 \mu\text{M}$ ) in  $50 \text{ mM}$  potassium phosphate (pH 7.0) monitored by mass spectrometric and stopped-flow fluorescence studies. (a) Transformed mass spectra acquired after incubating V211Cf with cefoxitin at different time intervals. (b) Time course for the binding of V211Cf with cefoxitin monitored by ESI-MS analysis and stopped-flow fluorescence spectroscopy. The solid line represents the fluorescence trace, and the red squares represent the relative population of  $\text{ES}^*$  species ( $[\text{ES}^*]/[\text{E}_{\text{total}}]$ ).

values are slightly lower (~2-fold) in both mutant enzymes compared to the wild-type enzyme. Moreover, the  $k_{\text{cat}}$  value of the unlabeled V211C mutant is very similar to that of the fluorophore-labeled V211Cf mutant. These results indicate that substrate binding ability and catalytic activity of the P99 enzyme are largely restored after V211C mutation and fluorophore conjugation.

Fluorescence properties of V211Cf were then characterized by fluorescence spectroscopy. In  $50 \text{ mM}$  phosphate buffer, V211Cf emits fluorescence at  $517 \text{ nm}$  upon an excitation at  $498 \text{ nm}$  (Figure S2, Supporting Information). Figure 3 illustrates the effect of  $\beta$ -lactam antibiotics on the fluorescence of V211Cf. It was shown that addition of penicillin G and cephalothin triggers an increase in fluorescence intensity of V211Cf. In both cases, after the fluorescence modulation, the fluorescence intensity of V211Cf declines and eventually returns to its basal level. When overlapping these fluorescence traces with the UV absorption spectra which reveal the presence of the  $\beta$ -lactam substrate (as the amide bond of  $\beta$ -lactam absorbs UV light), it was found that the time of recovery of the fluorescence to basal level matches the time of disappearance of UV signal (substrate depletion;  $\sim 300 \text{ s}$  for penicillin G;  $\sim 50 \text{ s}$  for cephalothin). Therefore, the fluorescence signals show the dynamics of the hydrolytic action of V211Cf on penicillin G and cephalothin. In addition, since the substrate binding to enzyme's active site enhances the fluorescence of V211Cf and the release of product from the active site reverses the fluorescence enhancement, it is envisioned that the fluorescence changes of V211Cf pertain to the vacancy of the enzyme's active site and the fluorescein molecule of V211Cf can report the local environment change in its active site upon substrate/inhibitor binding.

**Fluorescence Mechanism of V211Cf.** The drug-sensing ability of V211Cf was examined by both ESI-MS and fluorescence spectroscopy, using cefoxitin as the substrate. This antibiotic is relatively resistant to the hydrolytic activity of class C  $\beta$ -lactamases,<sup>34</sup> and therefore, the binding of V211Cf with this antibiotic can be conveniently probed by ESI-MS and fluorescence spectroscopy over a wider time interval.

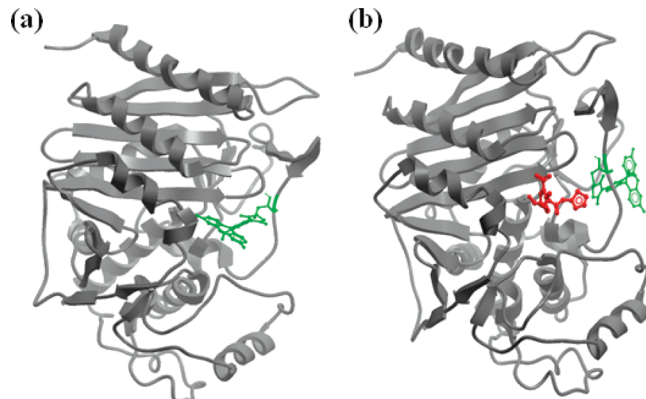


**Figure 5.** Molecular models of V211Cf with and without cefoxitin. (a) Stereoview of the active site of V211Cf in the free enzyme state. The fluorescein label (green) is buried inside the active site in this state. (b) Stereoview of the active site of V211Cf in the covalent  $\text{ES}^*$  state. The fluorescein label (green) stays out of the active site to make room for the cefoxitin molecule (red) in the  $\text{ES}^*$  state. The solvent accessible area of the fluorescein label in V211Cf increases from  $216$  to  $264 \text{ \AA}^2$  after substrate binding.

For ESI-MS analysis, briefly, V211Cf was incubated with cefoxitin, and the catalytic reaction was quenched at different time intervals by acid-unfolding of the labeled enzyme. Under these experimental conditions, the ES intermediate completely dissociates and the relative populations of the covalent  $\text{ES}^*$  complex at different time intervals can be detected. ESI mass spectra of V211Cf incubated with cefoxitin at different time intervals and the corresponding time profile of the formation of the complexes between V211Cf and cefoxitin are shown in Figure 4. As revealed in Figure 4b, the population of  $\text{ES}^*$  first increases, reaches a maximum at  $\sim 120 \text{ s}$ , and then gradually declines. This is ascribed to the hydrolytic process that V211Cf

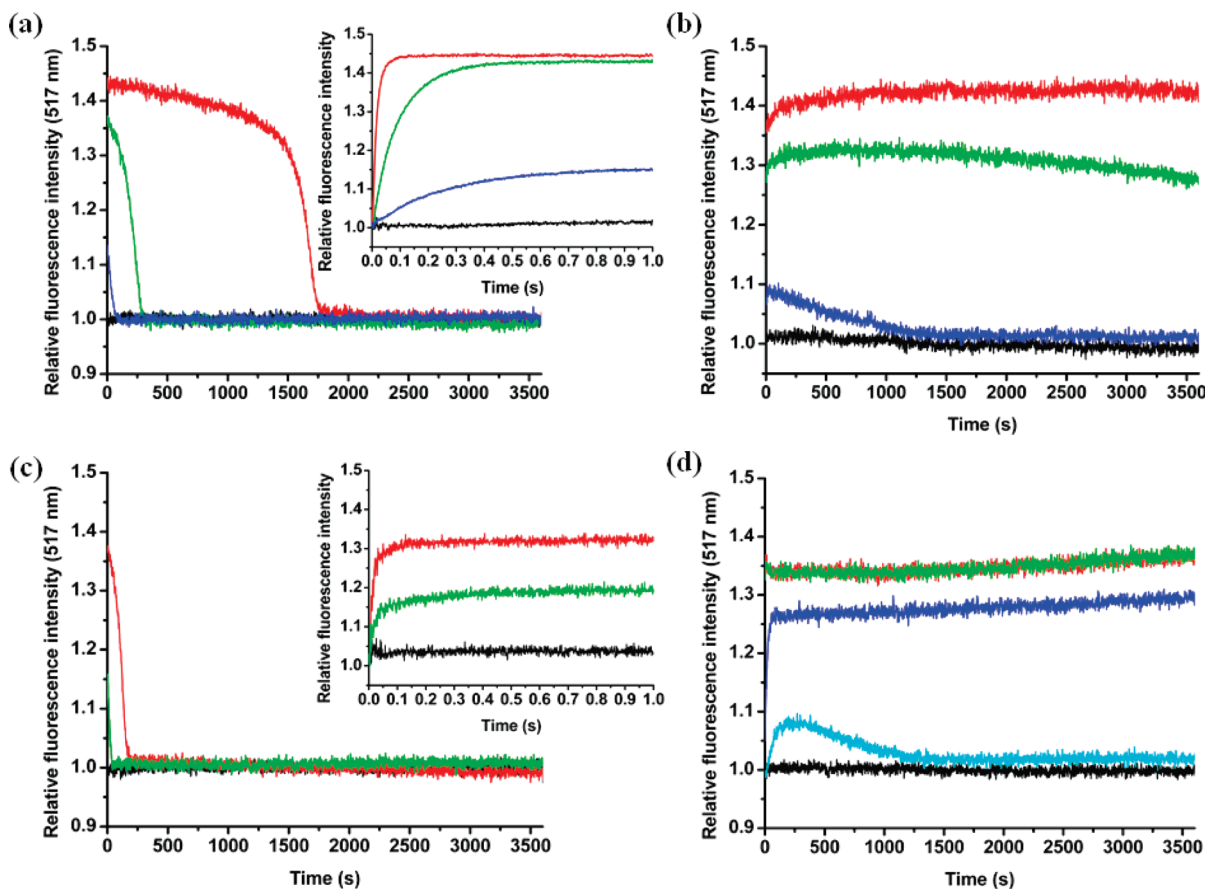


**Figure 6.** Steady-state fluorescence measurements of V211Cf with various  $\beta$ -lactam antibiotics. The fluorescence profiles for penicillin G, ampicillin, cephalothin, and cefoxitin are shown in (a–d), respectively. [Antibiotic]: 0 M (black);  $1.0 \times 10^{-6}$  M (cyan);  $1.0 \times 10^{-5}$  M (blue);  $1 \times 10^{-4}$  M (green);  $1.0 \times 10^{-3}$  M (red). [V211Cf]: 0.1  $\mu$ M. The insets in (a) and (c) show the fluorescence signals of V211Cf with different concentrations of penicillin G and cephalothin (respectively) recorded by stopped-flow fluorescence spectroscopy. Excitation wavelength: 498 nm; emission wavelength: 517 nm; buffer: 50 mM potassium phosphate (pH 7.0).

initially binds to cefoxitin to form covalent ES\* complex through acylation and then the ES\* complex dissociates to regenerate the enzyme's active site via deacylation.

When the time profiles obtained from the ESI-MS and fluorescence measurements (Figure 4b) are correlated, it is shown that the increase in the population of the ES\* state for cefoxitin is accompanied by the increase in fluorescence of V211Cf. Upon the addition of cefoxitin, the intensity of the fluorescence of V211Cf increases along with the formation of covalent ES\* complex until the maximum level of ES\* population is formed ( $t = 90 - 120$  s). Afterward, the fluorescence signal slowly declines to its basal level in accordance with the gradual dissociation of ES\* species. This indicated that the ES\* species prominently contributed to the fluorescence enhancement of V211Cf during the enzymatic hydrolysis of cefoxitin.

In order to investigate the mechanism of the substrate-modulated fluorescence enhancement of V211Cf, molecular models of V211Cf with and without cefoxitin are built (Figure 5). As revealed in Figure 5a, in the absence of cefoxitin (the E state), the fluorescein molecule orients its functional moiety in the enzyme's active site pocket with a solvent accessible area (SAA) of 216  $\text{\AA}^2$ . On the contrary, regarding the structure of V211Cf docked with cefoxitin (the ES\* covalent state; Figure 5b), cefoxitin occupies the enzyme's active site and the fluorescein molecule stays out from the active site. It is postulated that, upon binding to cefoxitin, in order to avoid the spatial clash of fluorescein with the functional group of cefoxitin, the

cefoxitin displaces the buried fluorescein molecule from the active site pocket to a more solvent exposed environment (SAA increases from 216 to 264  $\text{\AA}^2$ ). Thus, this conformational change of the fluorescein molecule results in the fluorescence enhancement of V211Cf, forming the drug-sensing basis of V211Cf.

**Fluorescence Behavior of V211Cf in the Presence of  $\beta$ -Lactam Antibiotics.** Figure 6 illustrates the time profiles of fluorescence response of V211Cf toward various  $\beta$ -lactam antibiotics. In general, the fluorescence signal consists of three phases: the rising phase, the plateau phase, and the declining phase. For example, for penicillin G, the fluorescence intensity of V211Cf increases instantaneously, levels off to a plateau, and then rapidly declines to its original level (Figure 6a). In addition, the fluorescence intensity, the rate of initial rise in the fluorescence signal, and the duration of fluorescence plateau increase as a function of antibiotic concentration. Furthermore, regarding the effect of substrates on the fluorescence of V211Cf, the stability of the substrate toward the hydrolytic action by the P99  $\beta$ -lactamase affects the pattern of the fluorescence signal. In the presence of rapidly hydrolyzed substrates, for instance, penicillin and cephalothin (for penicillin,  $k_{\text{cat}} = 4.5 \text{ s}^{-1}$ ; for cephalothin,  $k_{\text{cat}} = 47 \text{ s}^{-1}$ ), V211Cf displays a rapid initial fluorescence increase followed by a subsequent rapid recovery of its fluorescence to its basal level (Figure 6a,c). On the other hand, V211Cf shows a relatively slow initial rise in its fluorescence intensity and an extended period of the enhanced fluorescence with ampicillin and cefoxitin

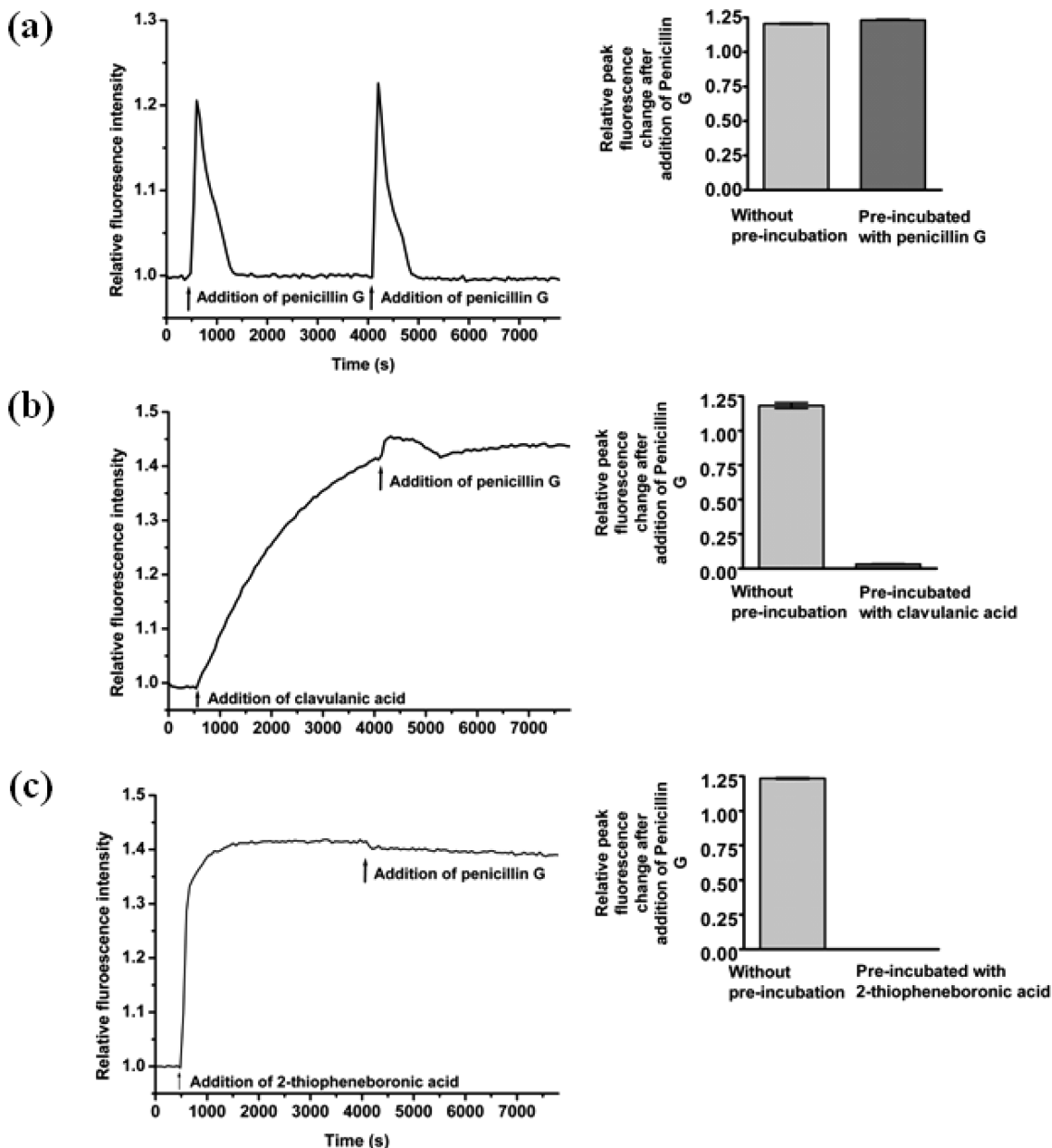


**Figure 7.** Drug screening assays with V211Cf monitored by a fluorescence microplate reader. The fluorescence profiles of V211Cf with penicillin G, clavulanic acid, and 2-thiopheneboronic acid are shown in (a–c), respectively. Penicillin G, clavulanic acid, and 2-thiopheneboronic acid were added to V211Cf ( $t = 420$  s), followed by the addition of penicillin G ( $t = 4020$  s). [V211Cf]: 0.1  $\mu$ M; [inhibitor]: 1 mM; [antibiotic]: 0.1 mM. The insets show the maximum fluorescence changes of V211Cf for penicillin G with and without preincubation with the inhibitors and antibiotic. Buffer: 50 mM potassium phosphate (pH 7.0). The error bars were obtained from three fluorescence measurements ( $n = 3$ ). Excitation wavelength: 485 nm; emission wavelength: 520 nm.

which are relatively resistant to the hydrolytic action by the P99  $\beta$ -lactamase (for ampicillin,  $k_{\text{cat}} = 0.2 \text{ s}^{-1}$ ; for cefoxitin,  $k_{\text{cat}} = 0.02 \text{ s}^{-1}$ ; Figure 6b,d). Taken together, the pattern and longevity of the fluorescence signal to the rate of hydrolysis by V211Cf which is governed by antibiotic type and concentration. As a result, the fluorescence profile can provide a track of the hydrolytic reaction in the real-time manner and delineate the stability of the antibiotic in the presence of P99  $\beta$ -lactamase.

**Specificity of V211Cf.** To evaluate the specificity of V211Cf in sensing the active site binding molecules, fluorescence measurements of V211Cf in the presence of agents that do not bind with the active site of the P99  $\beta$ -lactamase were conducted. From the results (Figure S3, Supporting Information), no observable

fluorescence signals are detected upon addition of glucose and antibiotics from other classes (including kanamycin and chloramphenicol). Besides, the specificity of V211Cf was assessed by adding Congo red, an aggregate-prone molecule. It has been reported that Congo red tends to form promiscuous aggregates at the concentration of 0.75 mM which can lead to nonspecific inactivation of class C  $\beta$ -lactamase's activity.<sup>35</sup> From the fluorescence readout, it is clearly observed that Congo red quenches the fluorescence of V211Cf instead of modulating a fluorescence increase of V211Cf. This remarkable difference in the fluorescence behavior of V211Cf toward Congo red and antibiotic substrates suggests that V211Cf can discriminate the active-site binding drug candidates from the nondruglike molecules.

**Application of V211Cf in Inhibitor Screening.** In order to demonstrate the ability of V211Cf to screen for inhibitors, we studied the fluorescence response of V211Cf with the combined inhibitor/antibiotic formulations: (1) clavulanic acid/penicillin G and (2) 2-thiopheneboronic acid/penicillin G. Briefly, V211Cf was first incubated with the inhibitors for  $\sim 1$  h, followed by the addition of penicillin G. The fluorescence of V211Cf was measured on a microplate reader over the time course. For comparison, similar experiments were also performed with V211Cf, except that the inhibitor was replaced with penicillin G.

We first investigated the inhibitory activities of clavulanic acid and 2-thiopheneboronic acid toward the wild-type P99 enzyme, V211C, and V211Cf by  $IC_{50}$  determination. Table S2 (Supporting Information) shows the  $IC_{50}$  values of clavulanic acid and 2-thiopheneboronic acid for the wild-type P99 enzyme, V211C, and V211Cf with nitrocefin as the substrate. For both clavulanic acid and boronic acid, the  $IC_{50}$  values for these three enzymes are similar, highlighting the high similarity in activity between the wild-type enzyme, V211C, and V211Cf. This indicates that V211Cf can replace the wild-type enzyme as a “natural” fluorescent drug target for *in vitro* drug screening. The  $IC_{50}$  value of 2-thiopheneboronic acid is, in general, lower than that of clavulanic acid for each enzyme. This observation is in good agreement with the fact that 2-thiopheneboronic acid is a stronger inactivator against the P99  $\beta$ -lactamase than clavulanic acid.<sup>36,37</sup>

The fluorescence response of V211Cf with clavulanic acid, 2-thiopheneboronic acid, and penicillin G were then studied. Figure 7 shows the time-course fluorescence profiles of V211Cf with the inhibitors and antibiotic. With penicillin G, which is very sensitive to the hydrolytic action of the P99  $\beta$ -lactamase, the fluorescence of V211Cf increases instantaneously upon injecting this antibiotic ( $t = 420$  s) and then declines rapidly (Figure 7a). The fluorescence enhancement can be attributed to the formation of enzyme–substrate complexes (ES and ES $^*$ ). The subsequent degradation of the ES $^*$  complex regenerates the free enzyme and hence restores the weak fluorescence of V211Cf. This implication is supported by the similar fluorescence profile generated by the second injection of penicillin G ( $t = 4020$  s). In both fluorescence profiles, the maximum fluorescence changes are virtually similar (Figure 7a: inset).

With clavulanic acid, the fluorescence of V211Cf increases gradually, indicating the binding of this inhibitor to the active site of V211Cf (Figure 7b). The subsequent addition of penicillin G ( $t = 4020$  s) causes V211Cf to increase its fluorescence weakly. This fluorescence enhancement ( $\sim 1.8\%$  increase) is much lower than that of V211Cf incubated with the same concentration of penicillin G in the absence of the inhibitor ( $\sim 18\%$  increase; Figure 7b: inset). The weak fluorescence enhancement is likely to arise from the competitive binding of clavulanic acid to the enzyme’s active site with penicillin G.

For 2-thiopheneboronic acid, similar observations were also obtained. The fluorescence of V211Cf increases rapidly to reach a plateau upon addition of 2-thiopheneboronic acid, indicating the binding of this inhibitor to the active site of V211Cf (Figure 7c). In this case, the fluorescence signal increases at a faster rate than that for clavulanic acid under similar experimental conditions, implying that thiopheneboronic acid binds more strongly to V211Cf than clavulanic acid (Figure 7b,c). This observation is consistent with the data obtained from the  $IC_{50}$  experiments; the  $IC_{50}$  value of thiopheneboronic acid for V211Cf is lower than that of clavulanic acid (Table S2, Supporting

Information). The subsequent addition of penicillin G ( $t = 4020$  s) does not cause a detectable fluorescence enhancement, implying that thiopheneboronic acid competes strongly with penicillin G for the active site of V211Cf.

When one takes the observations into consideration, V211Cf can detect inhibitors in a 96-well plate format and also reveal the potency of the inhibitors. In addition, in a clinical setting,  $\beta$ -lactam antibiotics are often used in combination with  $\beta$ -lactamase inhibitors so as to ensure the effectiveness of the  $\beta$ -lactamase-sensitive antibiotics in antibacterial treatment.<sup>38</sup> With the ability to differentiate the inhibitor’s potency, V211Cf can also become a screening platform that helps select an appropriate inhibitor partner for the  $\beta$ -lactam antibiotics for the drug formulation.

## CONCLUSIONS

The rapid emergence of antibiotic-resistant bacteria has been well-recognized as a non-negligible threat to human health. This clinical problem is primarily caused by the widespread ability of producing  $\beta$ -lactamases among various pathogenic bacteria. In particular, class C  $\beta$ -lactamases have received increasing recent attention because of their ability to efficiently hydrolyze cephalosporins, which are useful antibiotics in antibacterial therapies, as well as the lack of commercially available effective  $\beta$ -lactamase inhibitors. To combat this clinical problem, it is necessary to invent new therapeutics against these clinically important enzymes. In addition, examination of the inhibitory activities of these drug candidates *in vitro* can provide valuable insights into the structure-based design of new drugs with improved potency.

The fluorescent V211Cf mutant developed in this work represents an ideal protein-based drug screening platform for this purpose. This labeled mutant enzyme was strategically engineered in such a way that it can directly detect the binding of inhibitors/antibiotics to the active site while maintaining its catalytic activity close to the wild-type level, thus allowing itself to act as a “natural” fluorescent drug target for *in vitro* drug screening. Moreover, on the basis of our results, V211Cf is specific to its active site binding molecules. This feature enables V211Cf to be an effective screening tool that can eliminate false positives attributed to nonspecific binding compounds and aggregation-prone molecules. Furthermore, the fluorescent V211Cf mutant is compatible with microplate-based drug screening, which allows high-throughput drug discovery. With these advantageous properties, the fluorescent V211Cf mutant will undoubtedly find its application in the pharmaceutical industry and facilitate the discovery of new therapeutics against the clinically significant class C  $\beta$ -lactamase producing bacteria.

## ASSOCIATED CONTENT

**S Supporting Information.** Experimental section, Table S1 showing mass spectrometric data, Table S2 showing  $IC_{50}$  data, Figure S1 showing ESI mass spectra, Figure S2 showing excitation and emission spectra, and Figure S3 showing steady-state fluorescence measurements. This material is available free of charge via the Internet at <http://pubs.acs.org>.

## AUTHOR INFORMATION

### Corresponding Author

\*Phone: 852-3400-3977 (K.-Y.W.); 852-3400-8661 (Y.-C.L.). Fax: 852-2364-9932 (K.-Y.W.); 852-2364-9932 (Y.-C.L.). E-mail: bckywong@polyu.edu.hk (K.-Y.W.); bctleung@polyu.edu.hk (Y.-C.L.).

## ■ ACKNOWLEDGMENT

This work was supported by the Research Grants Council (PolyU 5463/05M), the Area of Excellence Fund of the University Grants Committee (AoE/P-10/01), and Central Research Grants of the Hong Kong Polytechnic University (G-T341, G-YH79, and A-PE70). We thank Dr. Ka-Fai Yiu, Dr. Yu-Wai Chen, Dr. Yanxiang Zhao, and Dr. Wai-Hong Chung for useful discussion.

## ■ REFERENCES

- (1) Fisher, J. F.; Meroueh, S. O.; Mobashery, S. *Chem. Rev.* **2005**, *105*, 395–424.
- (2) Ambler, R. P. *Philos. Trans. R. Soc., B: Biol. Sci.* **1980**, *289*, 321–331.
- (3) Jacoby, G. A. *Clin. Microbiol. Rev.* **2009**, *22*, 161–182.
- (4) Mustafi, D.; Hofer, J. E.; Huang, W.; Palzkill, T.; Makinen, M. W. *Spectrochim. Acta, Part A: Mol. Biomol. Spectrosc.* **2004**, *60*, 1279–1289.
- (5) Wilke, M. S.; Lovering, A. L.; Strynadka, N. C. J. *Curr. Opin. Microbiol.* **2005**, *8*, 525–533.
- (6) Tenover, F. C. *Am. J. Med.* **2006**, *119*, S3–S10.
- (7) Maiti, S. N.; Philips, O. A.; Micetich, R. G.; Livermore, D. M. *Curr. Med. Chem.* **1998**, *5*, 441–456.
- (8) Payne, D. J.; Du, W.; Bateson, J. H. *Expert Opin. Invest. Drugs* **2000**, *9*, 247–261.
- (9) Buzzoni, V.; Blazquez, J.; Ferrari, S.; Calò, S.; Venturelli, A.; Costi, M. P. *Bioorg. Med. Chem. Lett.* **2004**, *14*, 3979–3983.
- (10) Morandi, S.; Morandi, F.; Caselli, E.; Shoichet, B. K.; Prati, F. *Bioorg. Med. Chem.* **2008**, *16*, 1195–1205.
- (11) Plantan, I.; Selic, L.; Mesar, T.; Anderluh, P. S.; Oblak, M.; Prezelj, A.; Hesse, L.; Andrejasic, M.; Vilar, M.; Turk, D.; Kocjan, A.; Prevec, T.; Vilfan, G.; Kocjan, D.; Copar, A.; Urleb, U.; Solmajer, T. *J. Med. Chem.* **2007**, *50*, 4113–4121.
- (12) Tan, Q.; Ogawa, A. M.; Painter, R. E.; Park, Y. W.; Young, K.; DiNinno, F. P. *Bioorg. Med. Chem. Lett.* **2010**, *20*, 2622–2624.
- (13) Tondi, D.; Morandi, F.; Bonnet, R.; Costi, M. P.; Shoichet, B. K. *J. Am. Chem. Soc.* **2005**, *127*, 4632–4639.
- (14) Tondi, D.; Powers, R. A.; Caselli, E.; Negri, M. C.; Blázquez, J.; Costi, M. P.; Shoichet, B. K. *Chem. Biol.* **2001**, *8*, 593–611.
- (15) Wyrembak, P. N.; Babaoglu, K.; Pelto, R. B.; Shoichet, B. K.; Pratt, R. F. *J. Am. Chem. Soc.* **2007**, *129*, 9548–9549.
- (16) Jadhav, A.; Ferreira, R. S.; Klumpp, C.; Mott, B. T.; Austin, C. P.; Inglese, J.; Thomas, C. J.; Maloney, D. J.; Shoichet, B. K.; Simeonov, A. *J. Med. Chem.* **2010**, *53*, 37–51.
- (17) Babaoglu, K.; Simeonov, A.; Irwin, J. J.; Nelson, M. E.; Feng, B.; Thomas, C. J.; Cancian, L.; Costi, M. P.; Maltby, D. A.; Jadhav, A.; Inglese, J.; Austin, C. P.; Shoichet, B. K. *J. Med. Chem.* **2008**, *51*, 2502–2511.
- (18) Coan, K. E.; Shoichet, B. K. *Mol. Biosyst.* **2007**, *3*, 208–213.
- (19) Coan, K. E.; Maltby, D. A.; Burlingame, A. L.; Shoichet, B. K. *J. Med. Chem.* **2009**, *52*, 2067–2075.
- (20) McGovern, S. L.; Shoichet, B. K. *J. Med. Chem.* **2003**, *46*, 1478–1483.
- (21) McGovern, S. L.; Helfand, B. T.; Feng, B.; Shoichet, B. K. *J. Med. Chem.* **2003**, *46*, 4265–4272.
- (22) Waley, S. G. *Biochem. J.* **1974**, *139*, 789–790.
- (23) Feng, B. Y.; Shoichet, B. K. *Nat. Protoc.* **2006**, *1*, 550–553.
- (24) Feng, B. Y.; Simeonov, A.; Jadhav, A.; Babaoglu, K.; Inglese, J.; Shoichet, B. K.; Austin, C. P. *J. Med. Chem.* **2007**, *50*, 2385–2390.
- (25) Chan, P. H.; Liu, H. B.; Chen, Y. W.; Chan, K. C.; Tsang, C. W.; Leung, Y. C.; Wong, K. Y. *J. Am. Chem. Soc.* **2004**, *126*, 4074–4075.
- (26) Chan, P. H.; So, P. K.; Ma, D. L.; Zhao, Y.; Lai, T. S.; Chung, W. H.; Chan, K. C.; Yiu, K. F.; Chan, H. W.; Siu, F. M.; Tsang, C. W.; Leung, Y. C.; Wong, K. Y. *J. Am. Chem. Soc.* **2008**, *130*, 6351–6361.
- (27) Beadle, B. M.; Trehan, I.; Focia, P. J.; Shoichet, B. K. *Structure* **2002**, *10*, 413–424.
- (28) Frère, J. M. *Mol. Microbiol.* **1995**, *16*, 385–395.
- (29) Lobkovsky, E.; Moews, P. C.; Liu, H.; Zhao, H.; Frère, J. M.; Knox, J. R. *Proc. Natl. Acad. Sci. U.S.A.* **1993**, *90*, 11257–11261.
- (30) Goldberg, S. D.; Iannuccilli, W.; Nguyen, T.; Ju, J.; Cornish, V. W. *Protein Sci.* **2003**, *12*, 1633–1645.
- (31) Tsang, M. W.; Leung, Y. C. *Protein Expression Purif.* **2007**, *55*, 75–83.
- (32) Joris, B.; De Meester, F.; Galleni, M.; Reckinger, G.; Coyette, J.; Frère, J. M.; Van Beeumen, J. *Biochem. J.* **1985**, *228*, 241–248.
- (33) Cech, N. B.; Enke, C. G. *Mass Spectrom. Rev.* **2001**, *20*, 362–387.
- (34) Galleni, M.; Amicosante, G.; Frère, J. M. *Biochem. J.* **1988**, *255*, 123–129.
- (35) McGovern, S. L.; Caselli, E.; Grigorieff, N.; Shoichet, B. K. *J. Med. Chem.* **2002**, *45*, 1712–1722.
- (36) Monnaie, D.; Frère, J. M. *FEBS Lett.* **1993**, *334*, 269–271.
- (37) Weston, G. S.; Blázquez, J.; Baquero, F.; Shoichet, B. K. *J. Med. Chem.* **1998**, *41*, 4577–4586.
- (38) Drawz, S. M.; Bonomo, R. A. *Clin. Microbiol. Rev.* **2010**, *23*, 160–201.